Jebur, AAJ, Atherton, W, Al Khaddar, RM and Loffill, E

 Artificial neural network (ANN) approach for modelling of pile settlement of open-ended steel piles subjected to compression load

http://researchonline.ljmu.ac.uk/id/eprint/10206/

Article

# Artificial Neural Network (ANN) Approach for Modelling of Pile Settlement of Open-ended Steel Piles Subjected to Compression Load

Ameer A. Jebur [a, *], William Atherton[b], Rafid M. Al Khaddar[b], and Ed Loffill[b]

[a] Department of Civil Engineering, Liverpool John Moores University, Henry Cotton Building, Webster Street, Liverpool L3 2ET, UK.
[b] Department of Civil Engineering, Liverpool John Moores University, Peter Jost Centre, Byrom Street, Liverpool L3 3AF, UK.
[*] E-mail: A.A.Jebur@2015.ljmu.ac.uk; ameer_ashour1980@yahoo.com, Tel.: 0044(0)7435851479

## Abstract

This study was devoted to examine pile bearing capacity and to provide a reliable model to simulate pile load-settlement behaviour using a new artificial neural network (ANN) method. To achieve the planned aim, experimental pile load test were carried out on model open-ended steel piles, with pile aspect ratios of 12, 17 and 25. An optimised second order Levenberg-Marquardt (LM) training algorithm has been used in this process. The piles were driven in three sand densities; dense, medium, and loose. A statistical analysis test was conducted to explore the relative importance and the statistical contribution (Beta and Sig) values of the independent variables on the model output. Pile effective length, pile flexural rigidity, applied load, sand-pile friction angle and pile aspect ratio have been identified to be the most effective parameters on model output. To demonstrate the effectiveness of the proposed algorithm, a graphical comparison was performed between the implemented algorithm and the most conventional pile capacity design approaches. The proficiency metric indicators demonstrated an outstanding agreement between the measured and predicted pile-load settlement, thus yielding a correlation coefficient (R) and root mean square error (RMSE) of 0.99, 0.043 respectively, with a relatively insignificant mean square error level (MSE) of 0.0019.

**Keywords:** artificial neural network; sandy soil; steel open-ended pile; L-M algorithm; pile capacity.

## 1. Introduction

Pile foundations, are part of structural elements underneath superstructures, frequently utilised as a load transferring system through inadequate sub-soil layers into stiff bearing strata with high efficiency (McVay et al., 1989; Chen and Kulhawy, 2002; Tschuchnigg and Schweiger, 2015). Therefore, the stability and safety of structures supported by pile foundations relies largely on accurate assessment of the pile bearing capacity. Thus, numerous experimental and numerical methods in the geotechnical literature have been undertaken to explore the

35  behaviour of pile load-settlement. Steel open-ended piles are normally utilised to facilitate pile installation process

36  in preference to closed ended piles (Lehane and Gavin, 2001). Accurate assessment of the load carrying capacity

37  of a single pile is an important aspect and plays a key role in the pile foundation design process. However, pile

38  bearing capacity and associated settlement design procedures have traditionally been carried out separately.

39  Moreover, it has been claimed by Fellenius (1988) that *"the pile allowable load should be governed by a combined*

40  *approach considering pile settlement and soil resistance intemperately acting together and influencing the value*

41  *of each other,"* In relation to a pile settlement analysis, Poulos and Davis (1980); Vesic (1977) and Das (1995)

42  demonstrated that the elastic settlement could contribute the major part of the final pile settlement. Moreover, For

43  piles penetrated in sandy soil, elastic settlement accounts for total final settlement (Murthy, 2002). Precise

44  modelling of the pile load carrying capacity requires an accurate understanding of the load-settlement mechanism

45  along the embedded pile effective depth, which is indeterminate  and complex to quantify (Reese et al., 2006).

46

47  The load-settlement curve can be plotted only by performing full-scale pile load-tests. Alternatively, ultimate pile

48  capacity can be determined by conducting in-situ tests including the cone penetration test (CPT), dilatometer test,

49  standard penetration test (SPT) and the pressure meter test. Cost considerations and practical problems involved

50  in the testing process obliged researchers to provide alternative methods to determine the pile-load settlement

51  behaviour.

52

53  Pile capacity can also be predicted using several empirical formulae and conventional design frameworks, for

54  instance those proposed by Das (1995); Vesic (1967); and Poulos and Davis (1980). Due to many uncertainties,

55  these existing techniques provide oversimplification the problem by the incorporating several hypotheses

56  associated with the parameters that govern the load-settlement response (i.e. soil stress history, initial boundary

57  conditions (IBs), non-linear soil stress-strain relationship, method of pile installation, type of the pile testing,

58  theory of the pile critical depth). Furthermore, Fleming (1992) developed a new approach to analyse and predict

59  pile settlement under maintained loading using hyperbolic functions. It is an attempt to characterise the nonlinear

60  behaviour of base-soil and shaft-soil interaction. In this method, the contribution of mobilised skin friction, and

61  pile end-bearing capacity can be determined individually. Through the changing slope of such functions, the

62  developed approach reflects well in the increase of soil modules at low strain level. To demonstrate the accuracy

63  of the propose method, some examples were provided from back analysis of pile load test results for instrumented

64  model piles tested at different soil types.

65    Łodygowski and Sumelka (2006) criticised the numerical approaches regarding their reliability and validity since

66    simulation constitutive models can be sensitive to problem boundary conditions (i.e., stresses distributions).

67    Therefore, most of the available methods fail to gain reliable success regarding precise prediction of the pile

68    capacity and the corresponding settlement (Momeni et al., 2014; Loria et al., 2015; Jebur et al., 2017).

69

70    Recently, the application of the artificial neural network has been applied successfully by many researchers to

71    solve a wide range of engineering problems with satisfying performance (Al-Gburi et al., 2016; Asteris et al.,

72    2016; Ardakani and Kordnaeij, 2017; Derbal et al., 2017). Among those, Najafzadeh (2015) developed neuro-

73    fuzzy (NF-GMDH) approach enhanced by gravitational search algorithm (GSA) and particle swarm optimisation

74    (PSO) to the scour depth of groups of piles under the condition of clear water. Nine individual input parameters

75    (IIPs), at different contributions level, have been considered to develop and train the developed algorithms. The

76    learning stages efficiency for both model NF-GMDH-PSO, and NF-GMDH-GSA has been explored. The results

77    shown that the NF-GMDH-PSO model produced substantial agreement between the measured and the predicted

78    values with a correlation coefficient of 0.95, thus in parallel with a relatively negligible RMSE of 0.036. Soon

79    after, Najafzadeh et al. (2016) investigated the feasibility of different types of artificial intelligence (AI) methods

80    including model tree (MT), evolutionary polynomial regression (EPR) to predict the maximum scour depth of

81    bridge piers. The aforementioned predictive models were developed using dataset published in literature. The

82    efficiency of the trained models has been assessed using different measuring performance indexes. The result

83    revealed that the suggested MT model provides higher prediction accuracy compared to the GEP and EPR with

84    RMSE and MAE of 0.241 and 0.178, respectively.

85

86    Moreover, Najafzadeh et al. (2017) applied a new approach so called NFF-GMDH to assess the pier scour depth.

87    A total of 243 experimental dataset, encompassing several input variables and outputs, was used to train the

88    proposed network. The study results demonstrated that the proposed NFF-GMDH-PSO is more efficient compared

89    to the NFF-GMDH-GA and NFF-GMDH-GSA, and has the ability to predict the scour depth with remarkable

90    accuracy. This was confirmed by root mean square error and scatter index of 0.388 and 0.343, respectively.

91    Harandizadeh et al. (2018) explored the feasibility of three types of artificial intelligence methods to predict

92    ultimate pile bearing capacity subjected to a wide range of axial loads. In total, a database of 100 concrete and

93    steel piles were collected to implement the ANNs models. Four individual inputs parameters has been selected to

94    be used in the input space, including piles geometric properties, soil characterisation, angle of internal friction,

95     and number of hammer blows, and the model output was pile bearing capacity. The study results revealed that the

96     radial base function model had the ability to learn 98.9% of the measured values compared to Bayesian regulation

97     and the Levenberg-Marquardt training algorithms with correlation coefficient of 98.4%, and 93%, respectively.

98

99     Although many studies highlighting the application of artificial neural networks in deep foundations research, the

100    slow rate of convergence and getting trapped in local minima have been cited as the major drawbacks associated

101    with the conventional current ANN applications (Momeni et al., 2014; Rezaei et al., 2016). Therefore, a

102    comprehensive experimental study investigating the load-settlement response of steel model piles, including a

103    wide range of sand densities, conducted to create an accurate dataset to develop and run a new Levenberg-

104    Marquardt (LM) algorithm, would be a breakthrough, in pile foundation studies. Unlike conventional training

105    methods, the trained LM has several distinctive merits in that it is self-tuning training (doesn't require user

106    dependent parameters after each application), it is 10 to 100 times faster without being trapped in local minima,

107    less vulnerable to overfitting issues, has the ability to determine the optimum solution during the learning process,

108    and it is extremely recommended as the first choice of supervised algorithm. (Abdellatif, 2013; Alrashydah and

109    Abo-Qudais, 2018; Jebur et al., 2018b).

110

## 2. Aims and objectives

112    The current study has been conducted to fill a gap in literature with the aim of providing and accurate predictive

113    model. The objectives of the project were to:

114    • Carry out a series of experimental pile load-tests on steel open-ended piles with slenderness ratios ($l_c/d$)

115        of 25, 17, and 12 penetrated in three sand relative densities of dense, medium, and loose to investigate

116        the pile bearing capacity and to create a reliable laboratory dataset to develop the ANN model.

117    • Utilise a new Levenberg-Marquardt (LM) training algorithm, based on the MATLAB environment, to

118        develop the predictive model to establish if it can be successfully used to simulate pile capacity and

119        corresponding settlement.

120    • Develop a statistical model to explore the relative importance and the statistical significance ('Beta' and

121        'Sig') values of the independent variables (IVs) on the model output utilising the SPSS-23 package.

122    • Compare the newly applied LM algorithm performance with the most commonly used pile bearing

123        capacity approaches.

124

## 3. Implementation and mathematical background of the LM algorithm

The feasibility of the LM training algorithm has recently been underlined as an efficient prediction tool in many engineering sectors and is now gaining growing attention in engineering research (Deo and Şahin, 2015; Juncai et al., 2015; Jebur et al., 2018b). These technical papers have reported the outstanding performance of the LM algorithm over the classical artificial neural networks methods. It should be stressed that one of the obvious advantages of the LM method is that no training parameters are required to be modified for the trained algorithm, thus avoiding many difficulties and barriers noted by the use of other ANN algorithms parameters such as the momentum term, learning epochs (an epoch is a single step or one complete presentation of the data-set to be trained during the iteration process), learning rate and local minima (Deo and Şahin, 2015). Furthermore, the introduced LM algorithm has been certified to be several times faster and stable training algorithm in comparison to other conventional machine learning algorithms (i.e., support machine vector) (Wilamowski and Yu, 2010; Rajesh and Prakash, 2011; Jebur et al., 2018a). Therefore, the LM training algorithm has been considered as a superior data-driven algorithm to provide accurate solutions for complex non-linear problems such as the one considered in the current study.

The basic theory of the LM model reveals that for M input model parameters $(x_k, y_k) \in R^m R^m$, the feedforward based on standard single layer with N hidden neurons and an activation function $g(.)$ can be described in equation 1:

$$\sum_i^n B_i g\left(x_k, ; c_i, a_i\right) = y_k \qquad \text{where } K = 1, 2, \dots \dots \dots \dots M \qquad (1)$$

where $K = 1, 2, \dots \dots \dots \dots M$

$c_i \in R$ is the bias of the $i$th hidden nodes that are randomly assigned during the training process, $w_i \in R$ is the weight assigned to each of the model input parameters connecting the $i$th model input parameters to the hidden neurons or nodes. It should be noted that this is not constant and is modified for each training process. $B_i$ is the weight vector used to connect the $i$th hidden node to the corresponding output node, $g(x_k, ; c_i, a_i)$ is the hidden node output with respect to the model input. Each model input parameter is indiscriminately allocated to the hidden nodes. Consequently, Eq. 1, can be rewritten as below:

$$HB = Y \qquad (2)$$

154     where

$$H = \begin{bmatrix} g(x_1,; c_1,; w_1) & g(x_1,; c_n,; w_n) \\ g(x_1,; c_1,; w_1) & g(x_1,; c_n,; w_n) \end{bmatrix} M.N \tag{3}$$

$$HB = (B_1^T\ B_2^T, \dots, B_l^T)_{n.N}^{T} \tag{4}$$

155

156     And the output $(Y)$

157

$$Y = (t_1^T\ t_2^T, \dots, t_l^T)_{n.N}^{T} \tag{5}$$

158

159     It should be highlighted that the output weights are determined by determining the least square solution to the

160     linear system, as described below:

161

$$B = H^{+}Y \tag{6}$$

162

163     $H^{+}$ is the Moore-Penrose generalised inverse of the matrix H. the bias and the input weight are randomly selected.

164

165     After briefly describing the LM algorithm basic theory, the development of the LM training algorithm requires

166     the definition of the model inputs and output, pre-processing and division of the dataset, the selection of the

167     optimum network and stopping criteria (Shahin and Jaksa, 2005). In this investigation, a new Levenberg-

168     Marquardt (LM) algorithm, was developed and trained based on the MATLAB environment, details about the

169     train algorithm code is provided in appendix A. Figure 1, illustrates the general LM training process. Furthermore,

170     the recorded database collected from experimental pile-load tests was utilised to develop and validate the LM

171     algorithm. 9 pile-load tests were conducted for model steel open-end piles with slenderness ratios ranged from

172     12, 17 and 25, driven in three sand relative densities, $D_r$ of loose medium and dense. Accordingly, the LM

173     algorithm based ANN model was established using the dataset that spanned the range of conditions that can be

174     found in different in situ conditions.

175
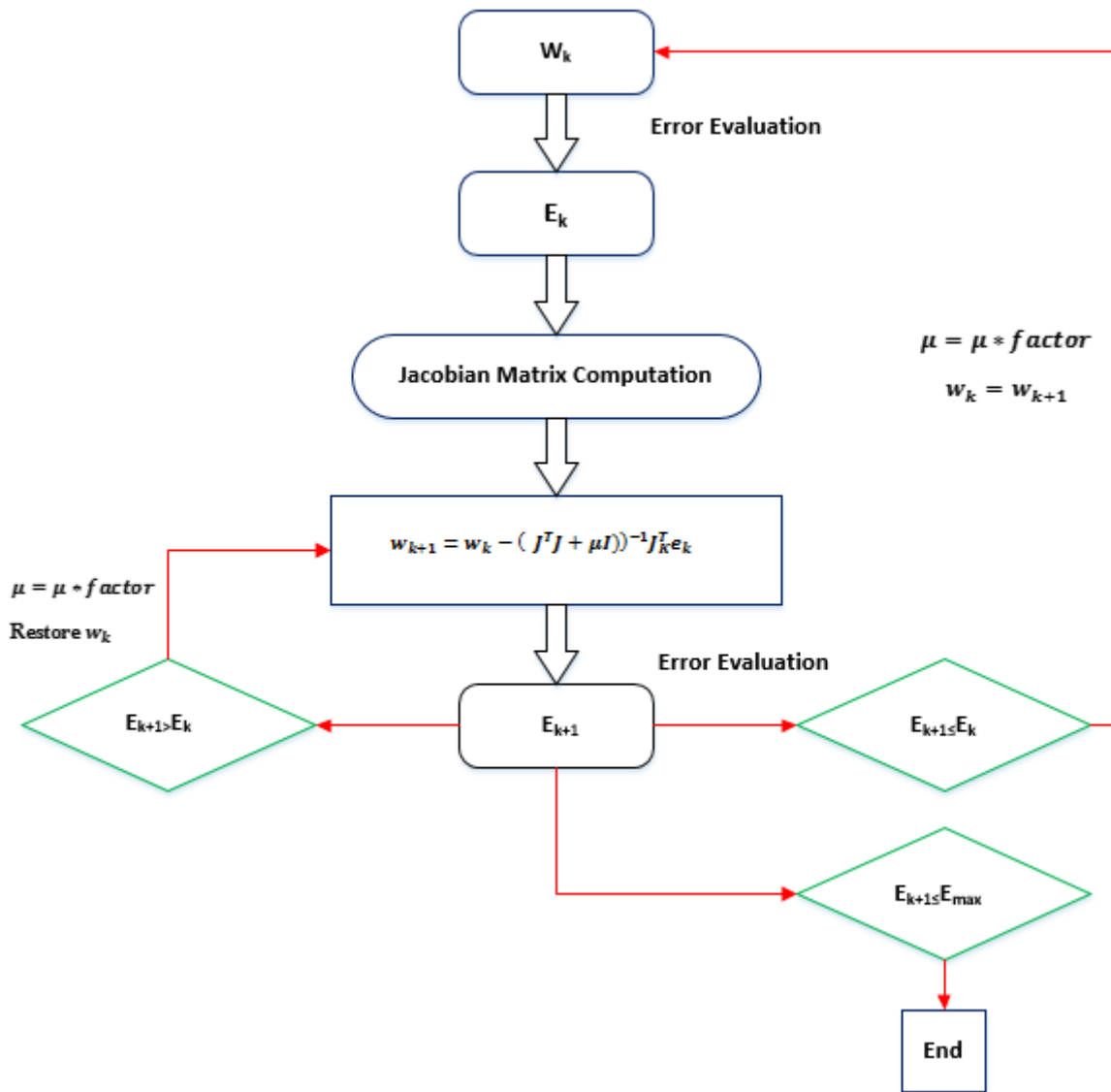
Figure 1. Block diagram displays the training process utilising the LM algorithm:

Where: $w_k$ denotes the existing weight, $w_{k+1}$ is the subsequent weight, $E_{k+1}$ and $E_k$ are the current and last total

error respectively.

## 4. Materials and methods

### 4.1. Sand characteristics

Uniform, fine sand with a quartz content of 97.4% was utilised in the test chamber. shape of the sand particle

along with the size can be considered as a significant factor effecting the shear behaviour of granular materials

(Dyskin et al., 2001). Cho et al. (2006) stated that decreasing sphericity and roundness or increasing angularity

leads to an increase in minimum ($e_{min}$) and maximum ($e_{max}$) void ratios of the sand. To this end. Figure 2 shows

that a scanning electronic microscopy (SEM) test at 137x magnification and a working distance (WD) of 26.2 mm

190    was used to examine the shape of the sand used in the experimental programme. It can be seen that the sand

191    particles consisted of sub-rounded particles, which leads to higher unit weight compared to rounded particles.

192    Following the unified soil classification system criteria, this sand can be classified as poorly graded (SP). The

193    sand density has been prepared in three types of loose (18%), medium (51%) and dense (83%), respectively.

194    Physical properties of the sand utilised in the testing program are summarised in Table 1. The shear strength

195    characteristics of the sand-sand angle, Ø and pile-sand angle, δ are experimentally measured using the direct shear

196    tests in accordance with the BSI (BS EN 1377-7:1990) standard. In order to minimise the scale effect, the impact

197    of the sand grain size distribution on the sand-pile interaction should be maintained. However, the pile diameter

198    (D) should be 60 times the medium diameter of the sand ($d_{50}$) (Remaud, 1999). Whereas, Taylor (1995) however,

199    stated that the minimum ratio must be 100. In the current study, the ratio between the diameter of pile to the sand

200    medium diameter ($d/d_{50}$) is 133 as revealed in Figure 3, satisfying the scaling law standard. To prepare the loose

201    sand bed, the sand particles were poured into the pile testing chamber by means of a tube delivery system, as

202    proposed by Schawmb (2009). The tube end is repeatedly held at a maximum set distance of about 40 mm between

203    the sand delivery tube and the surface test bed. While, the medium sand was prepared using an air pluviation

204    technique discussed by Ueno (2000). The sand density was controlled by the falling rate at about 800 mm above

205    the sand surface with an accuracy of ± 30 mm until the tested depth being achieved. In addition, the dense sand

206    beds were carefully prepared following the technique detailed by Akdag and Özden (2013).

207
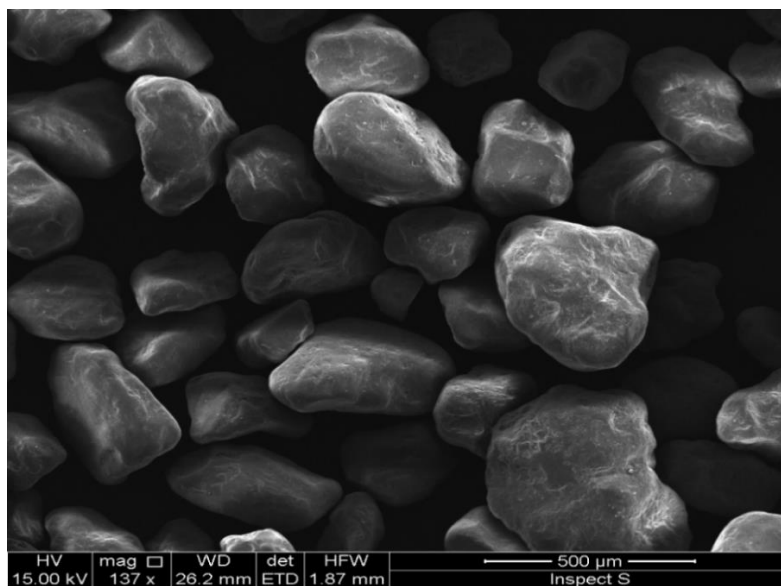


209    Figure 2. Scanning electronic microscopy (SEM) test of the sand particles.

210

211 where HV and mag stand for high voltage and magnification, WD, det, ETD, and HFW are, respectively, working

212 distance, detector, Everhart-Thornley detector, and horizontal field width.

213

214 Table 1. Properties of the sandy soil utilised in the experimental programme.

| Soil Property | Value |
|---|---|
| Uniformity Coefficient, Cu | 1.78 |
| Specific Gravity, $G_S$ | 2.62 |
| Coefficient of Curvature, Cc | 1.14 |
| Grain Size, $D_{10}$ (mm) | 0.22 |
| Mean Grain Size, $D_{50}$, (mm) | 0.34 |
| Pile-sand interface friction angle ($\delta$) for loose, medium, and dense sand | 17°, 17.7° and 19° |
| Maximum Index Unit Weight, $\gamma_{d\ max}$ (kN/m$^3$) | 17.45 |
| Minimum Index Unit Weight, $\gamma_{d\ min}$ (kN/m$^3$) | 15.34 |
| Maximum Index Void Ratio, $e_{max}$ (%) | 0.71 |
| Minimum Index Void Ratio, $e_{min}$ (%) | 0.49 |

215
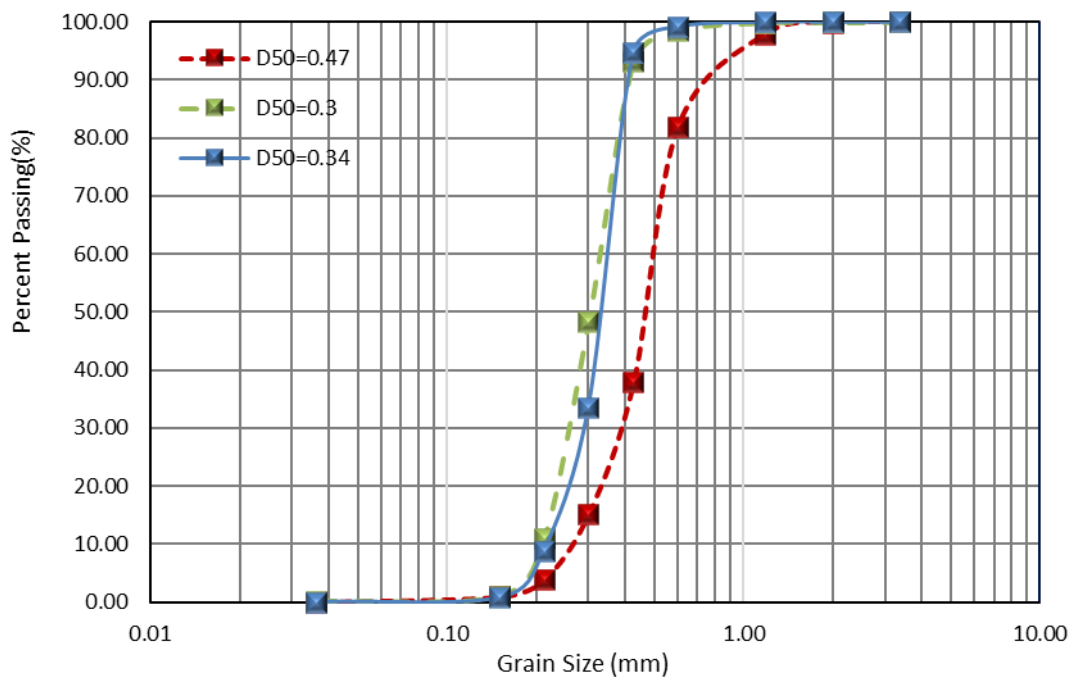


216
217 Figure 3. Particle size distribution of the sand sample.

218

## 4.2. Model piles and loading system

219

220  An experimental pile load-test program was carried out using the setup shown in Figure 4, to investigate the

221  bearing capacity of steel piles driven in sand soil. 40mm pile diameter with 1.2 mm wall thickness were utilised

222  in this study giving D/T ratio of 33.3 within the range of the D/t (15-45) as recommended by Jardine and Chow

223  (2007) for steel piles. The piles were tested in dry sandy soil. This assumption has been made due to the fact that

224  the capillary zone in sands is a relatively small, and thus is considered a lesser significance degree and can be

225  ignored (Józefiak et al., 2015). The piles were driven in a large calibration chamber with internal dimensions are

226  (900mm x 900mm x 1200mm length) and a wall thickness of 18mm. The pile effective lengths ($l_c$) were

227  considered of 480, 680, and 1000mm, giving embedment length-to-diameter ratios of 12, 17 and 25 were used to

228  examine the response of flexible, and rigid piles (Reddy and Ayothiraman, 2015). The model steel piles were

229  characterised by a Poisson's ratio, ν of 0.27 and E = 200GPa, which is highly comparable to the suggested material

230  values (195-210) GPa for steel piles subjected to compression loads (Gere and Timoshenko, 1997). The pile point

231  of loading was 50mm above the sand surface to minimise contact of the soil with the pile cap. This can help ensure

232  that the pile capacity is only due to soil-pile interaction. Regarding the loading procedure, a maintained load test

233  was run at loading rate of 1mm/min as specified by Bowles (1978) and within the limits stated by BSI (BS EN

234  8004:1986). The compression loads have been incrementally applied via a new hydraulic jack system attached at

235  the top to a load cell type (DBBSM) having 10kN capacity which was secured between the pile head loading

236  system and the hydraulic ram. Furthermore, the loads were applied directly on a pile cap manufactured from

237  aluminium with dimensions of 20mm thick and 150mm diameter. A spherical steel ball bearing was used on the

238  top of the pile cap to avoid eccentricity during the load application. The pile head displacement was monitored

239  using a data acquisition system instrumented with two linear variable differential transformers (LVDTs) of very

240  high resolution 0.01mm with 50mm travel to record the corresponding settlement. Using magnetic stands, the

241  LVDTs were located on the top of the pile cap in pairs so that bending effect could be accurately accounted for.

242

243

244

245



Double acting hydraulic ram

Loading frame (1.2m*3m)

Pile testing chamber (1m*1.5m)

Data logger (settlement recording system)

246
247                     Figure 4. Schematic view and dimensions of the experimental test setup.

248

249

## 4.3. Statistical analysis and dataset pre-processing

250

251    The dataset recorded from the experimental pile load-settlement tests was passed through three statistical steps to

252    develop a reliable ANN model (Tabachnick and Fidell, 2013). The total dataset needed to be tested to check the

253    statistical significance, the size of the dataset and residuals homoscedasticity, and to detect the presence of outliers

254    (Tabachnick and Fidell, 2013). Details about aforementioned tests are discussed in the following sub-sections.

255

256

### 4.3.1 Sensitivity analysis

Introducing a large number of model input parameters to developed an ANN leads to increase in the size of the network and the time required to precisely identify the optimum ANN model, thereby triggering a decrease in the processing speed (Rafiq et al., 2001) and thus leads to overfitting problems (Abdellatif et al., 2015). Therefore, a reliable analytical method to effectively identify the most significant input parameters and to highlight the level of significance of each parameter is needed. In this context, an innovative statistical analysis was conducted, using a multiple regression (MR) approach, to detect the model input variables (IVs) with the most influence and to underline the influence that a given IV has on the model output. The MR method has been applied because it has many attractive merits, such as its ability to examine the relationship between one individual variable (IV) with a set of other individual variables (IVs) (Jebur et al., 2018a).  Tabachnick and Fidell (2013) stated that any IV at Sig value > 0.05 could be omitted, as it has no significant influence on the suggested model. Based on the outcomes of the current statistical analysis, five factors, with different strengths of contribution, were highlighted as the most influential input parameters that govern the model output, as in Table 2. These parameters are (i) applied load, P, (ii) pile aspect ratio, lc/d, (iii) pile axial rigidity, EA, (iv) the sand-pile friction angle, $\delta$, and (v) pile embedded length, lc. Additionally, a sensitivity analysis was conducted to evaluate the contribution level of each IV on model output. Statistically, the closer to 1 the absolute Beta value, the more significant the influence of that IV on the model target (Pallant, 2005). Table 2 shows that the parameters P and $\delta$ have the highest level of contribution on the output with Beta values of 0.804, and 0.711, respectively.

Table 2. Results of the statistical analysis.

| IVs | Sig. value | Beta. value | Maximum MDs |
|---|---|---|---|
| Applied load, (P) | 0.000 | 0.804 | 17.63 |
| Sand-pile friction angle, ($\delta$) | 0.000 | 0.711 | |
| Flexural rigidity, (EA) | 0.010 | 0.015 | |
| Slenderness ratio, (lc/d) | 0.040 | 0.119 | |
| Pile length, (l) | 0.032 | 0.088 | |

### 4.3.2 Dataset size

According to Eq. 7, suggested by Tabachnick and Fidell (2013) and based on the number of the independent variables (IVs), the minimum number of dataset values required to develop a reliable model is 90. In the current study, a total of 274 points were collected experimentally. Thus, the condition of the data size has been met. A summary of the statistical parameters (i.e., Min, Max, S.D, and Mean) of the dataset are given in Table 3.

$$N > 50 + 8 * K \tag{7}$$

where: N and k are the total dataset and the number of the independent variables (IVs), respectively.

Table 3. A statistical summary of the characterisation of testing, training, and cross-validation dataset.

| Data Set | Statistical Parameters | Input Variables | | | | | Output |
|---|---|---|---|---|---|---|---|
| | | Load (kN) | Slenderness ratio Lc/d | Pile length, (m) | Pile axial rigidity, EA (MN) | Sand-pile friction angle, δ° | Settlement , (mm) |
| Training Set | Max. | 4.260 | 25 | 1 | 251.18 | 19 | 14.45 |
| | Min. | 0.002 | 12 | 0.48 | 251.18 | 17 | 0.002 |
| | Mean | 1.251 | 17.17 | 0.717 | 251.18 | 17.91 | 5.952 |
| | S.D.* | 1.202 | 1.342 | 0.210 | 0.00 | 1.04 | 4.435 |
| | Range | 4.458 | 13 | 0.52 | 0.00 | 2 | 14.45 |
| Testing Set | Max. | 4.256 | 25 | 1 | 251.18 | 19 | 14.35 |
| | Min. | 0.002 | 12 | 0.48 | 251.18 | 17 | 0.0165 |
| | Mean | 1.233 | 17.24 | 0.724 | 251.18 | 17.84 | 6.207 |
| | S.D.* | 1.342 | 0.138 | 0.226 | 0.00 | 1.047 | 4.665 |
| | Range | 4.254 | 13 | 0.52 | 0.00 | 2 | 14.34 |
| Validation Set | Max. | 4.261 | 25 | 1 | 251.18 | 19 | 14.18 |
| | Min. | 0.211 | 12 | 0.48 | 251.18 | 17 | 0.449 |
| | Mean | 1.240 | 17.365 | 0.725 | 251.18 | 17.83 | 7.011 |
| | S.D.* | 1.118 | 1.352 | 0.216 | 0.00 | 1.049 | 4.609 |
| | Range | 4.050 | 13 | 0.52 | 0.00 | 1.117 | 13.73 |

### 4.3.3 Outliers

Outliers can be illustrated as an observation point, that appears to be incompatible with other dataset observations (Walfish, 2006). The models generalisation ability can be highly affected by the existence of such extreme points. Consequently, all IVs and DVs must be checked in the pre-processing stage. Based on the statistical criteria suggested by Tabachnick and Fidell (2013), the presence of outliers could be examined using the Mahalanobis

295    distances (MDs). In this study, the maximum MDs must be less than the critical value 20.52 for five IVs (Pallant,

296    2005). The screening test demonstrated that the upper limit of the MDs was found at 17.63. While, for the

297    experimental data, the highest of the MDs was found to be 17.63, as given in Table 2, which confirmed the absence

298    of outliers in the studied observations.

299

300    **4.4. Development of the LM training algorithm**

301    One of the primary aims of this study was to develop the LM based ANN model to fully correlate the pile load

302    and corresponding settlement. The Levenberg-Marquardt (LM) training algorithm was used based on the

303    MATLAB environment, version (R2017a). ANN model topology was determined by a single layer, transfer

304    functions (TANSIG and PURELIN) and the number of nodes (neurons) in the hidden layer. Moreover,

305    optimisation of an ANN topology has been cited as the most important task in the ANN model development

306    (Tabachnick and Fidell, 2013). In total 9 pile load tests curves were carried out to examine pile bearing capacity

307    and to provide an accurate dataset to develop and train the proposed LM algorithm. In an attempt to identify the

308    optimum number of neurons, different ANN model structures has been used in terms of learnings and number of

309    hidden neurons. The minimum value of MSE associated with 10 hidden neurons. Therefore, the trained ANN

310    model with 10 neurons found to be the most appropriate structure for the developed model as illustrated in Figure

311    5.

312

313    In most recent studies, the percentage of the training sub-set is advised to fall within the range of 60% to 80%

314    from the total dataset (Alrashydah and Abo-Qudais, 2018; Jebur et al., 2018a). The training aim is to determine

315    the strength of the trained network by constructing the connection weights and threshold bias for the model input

316    and output parameters. The testing subset was piloted to check the reproducibility and the generalisation ability

317    of the proposed algorithm. The cross-validation subset was located to assess the model performance, terminate

318    the learning process, and to avoid overfitting at a minimum value of the mean square error (MSE) (Tarawneh,

319    2017). The process of learning utilized was back-propagation, and the resulting biases and weights of the best-fit

320    trained LM algorithm are provided in Appendix B.

321

322    In this study, the optimum ANN structure was identified as one single hidden layer with transfer functions of

323    tangent sigmoid (TANSIG) and linear (PURELIN) for the hidden and output layers respectively, as presented in

324    Eqs. 8, and 9, respectively. According to the statistical analysis study, five independent variables (IVs) were

specified as the most significant input parameters affecting pile bearing capacity. These parameters were applied load (P), pile aspect ratio (lc/d), pile effective length (lc), pile axial rigidity (EA), and the sand-pile angle of friction ($\delta$). The model output was the pile settlement. It is worth noting that the optimal structure of the LM based artificial neural network (ANN) has been selected at topology of 5:10:1 as revealed in Figure 6. The database values were scaled between 0.0 and 1.0, before being processed, to be given equal attention during the network training process and to minimize the ANN model ill-conditioning (Masters, 1993; Cho, 2009; Majeed et al., 2013). As part of this process, for each parameter with maximum, and minimum values of $X_{max}$ and $X_{min}$, the definition of the "normalised" value, $X_n$, can be evaluated using Eq. 10. The training parameters utilised are: (i) Learning rate: 0.001, (ii) Momentum: 0.100, (iii) Maximum number of iteration: 1000, and (iv) desired summation sequare error (SSE): 0.01.

$$Z_j = \frac{1}{1 + \exp\left(\sum_{i=1}^{n} \pm w_{ij}^{(1)} x_i \pm b_j^{(1)}\right)} \tag{8}$$

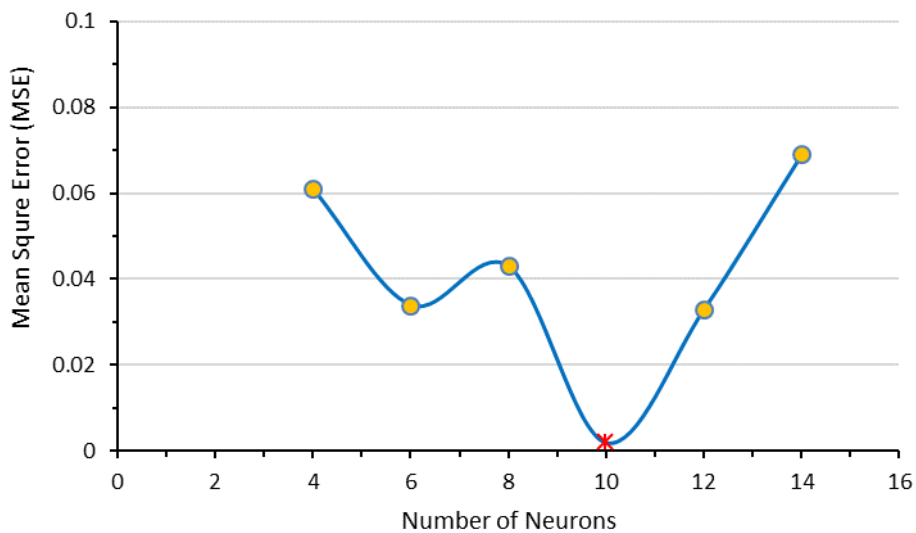$$y = \sum_{i=1}^{n} w_j^{(2)} z_j \pm b^{(2)} \tag{9}$$

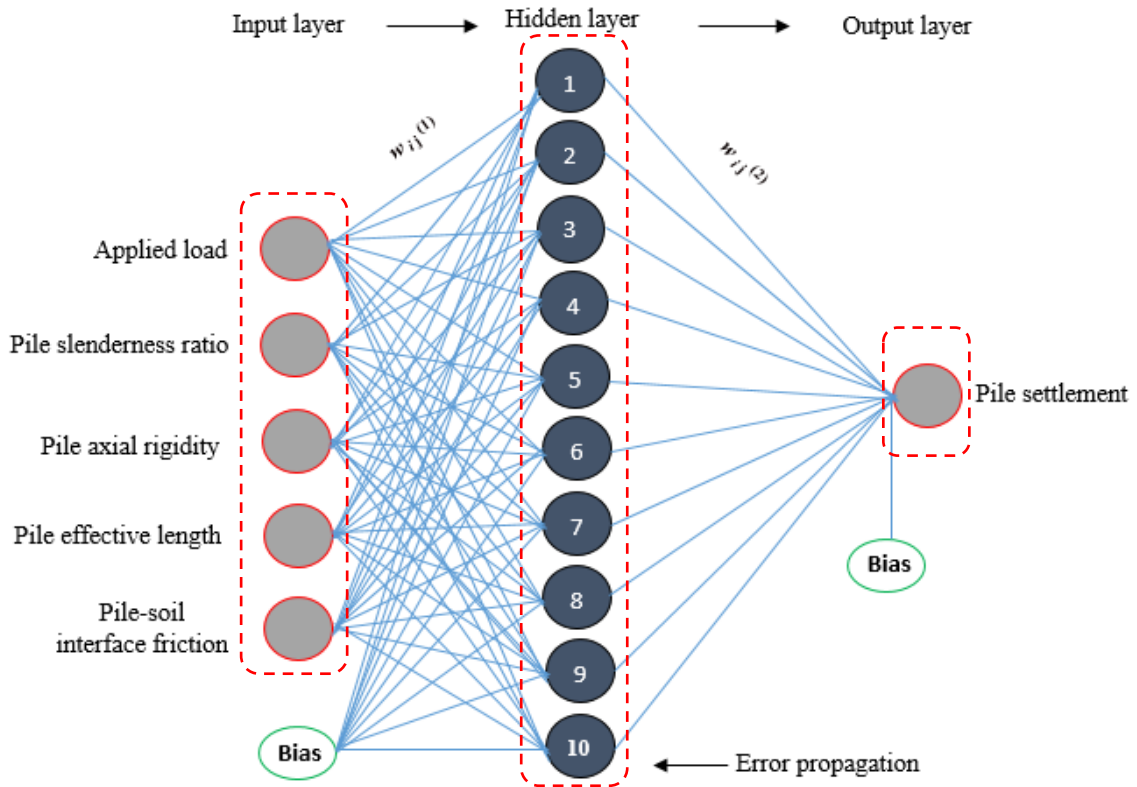$$x_{norm} = \frac{x_i - x_{i\,(min)}}{x_{i\,(max)} - x_{i\,(min)}} \tag{10}$$

where: the factors $w_{ij}^{(1)}$ and $b_j^{(1)}$ are the synaptic connection weights and biases from the inputs and hidden layer; $b_i^{(1)}$ and $b_i^{(2)}$ are the assigned bias for the layer one and two.



Figure 5. Shows variation effect of number of neurons in the hidden layer on mean square error (MSE).

341



342
343 Figure 6. Optimised ANN model inputs and output.

344

345

346 **4.5. Results and discussion**
347
348 **4.5.1 The LM algorithm measuring performance**

349 The measuring accuracy indicators of the trained LM algorithm was firstly assessed during the learning or training

350 process. The aforementioned training algorithm was used, as it is a most efficient and reliable method amongst

351 all other feedforward artificial intelligence (AI) methods (Jeong and Kim, 2005; Nguyen-Truong and Le, 2015).

352 The optimum model performance was statistically evaluated utilising the following metric skill with an error value

353 goal set at 0.01: mean square error (MSE), correlation coefficient (R) and root mean square error (RMSE)

354 functions as listed in Eqs. 11, 12 and 13, respectively, as they are the main standards that are utilised to measure

355 the network performance (Erdal, 2013).

356

357

$$MSE = \frac{\sum_{i=1}^{n}(O_i - t_i)^2}{n} \tag{11}$$

$$R = \frac{\sum_{i=1}^{n}(O_i - t_i)}{\sum_{i=1}^{n}(O_i - O_{mean})} \tag{12}$$

$$RMSE = \sqrt{\frac{1}{n}\sum_{i=1}^{n}(O_i - t_i)^2} \tag{13}$$

$$BIAS = \frac{\sum_{I=1}^{n}(O_i - t_i)}{n} \tag{14}$$

$$SI = \frac{RMSE}{(1/n)\sum_{i=1}^{n}t_i} \tag{15}$$

358

359    in which n stands for the total number of dataset, $O_i$ and $t_i$ are, respectively, the predicted and targeted values,

360    $O_{mean}$ is the average of the network output.

361

362    The measuring performance of the employed LM algorithm under the training process is demonstrated in Figure

363    7, it can be noted that the optimum model performance was identified at the minimum square error (MSE),

364    alternatively known as the performance index of 0.0019152 at an epoch of 389. It can also be seen that the model

365    performance is tested at many stages and the training was stopped with minimum MSE to avoid overfitting and

366    to improve the generalisation ability of the proposed algorithm once the cross validation subset started to increase.

367    This method is called early stopping criteria (Shawash, 2012).

**Best Validation Performance is 0.0019152 at epoch 389**
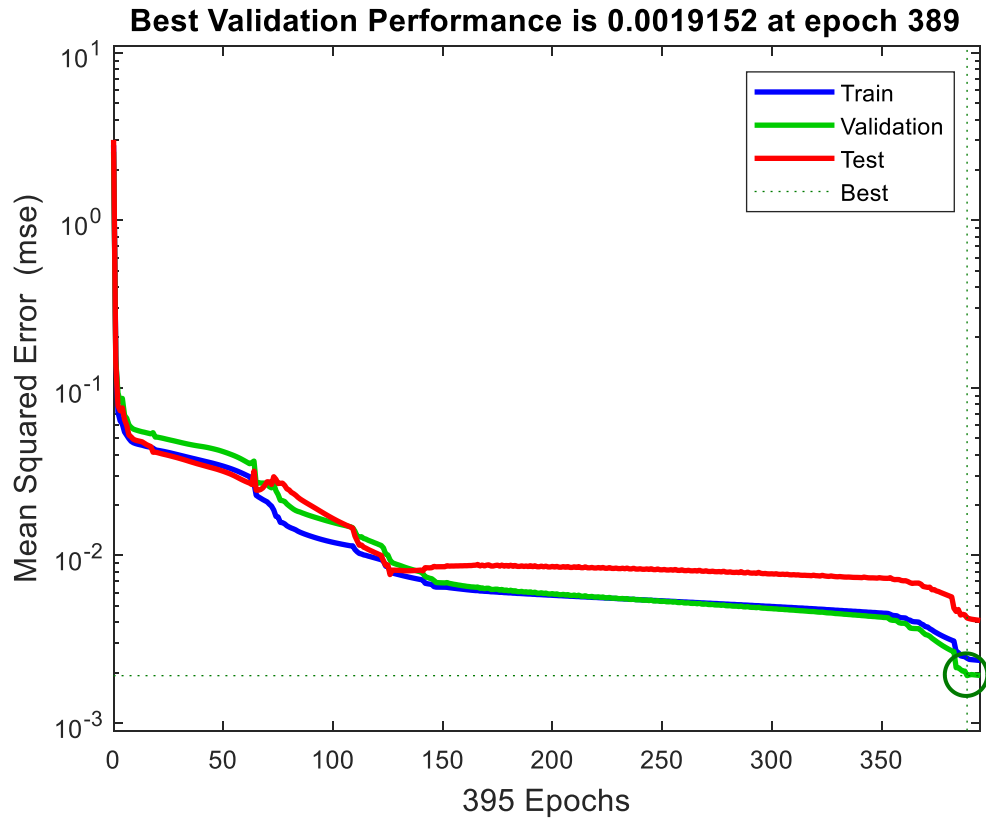
368

369                Figure 7. Performance profile of the LM algorithm during the training process.

370

371     Moreover, the error gradient variation, the Marquardt adjustment ($m_u$) and the validation checks are demonstrated

372     in Figure 8. It can also be shown that the gradient error was 0.00010525, while, the $m_u$ factor and the validation

373     check were $1*10e^{-05}$ and 6 at an epoch of 395. Moreover, Figure 9, presents the error histogram graph (EHG) to

374     obtain additional efficiency validation of network performance. The EHG can give an indication of outliers and

375     data features that appear to be inconsistent with other subsets observations (Yadav et al., 2014; Abdellatif et al.,

376     2015). It should be highlighted that the conclusions from the training can be extremely effected by outliers

377     (Tabachnick and Fidell, 2013). Thus, the training process is stopped once the validation error starts to increase.

378     In addition, it can be shown that the majority of dataset coincides with the line of zero error.

379
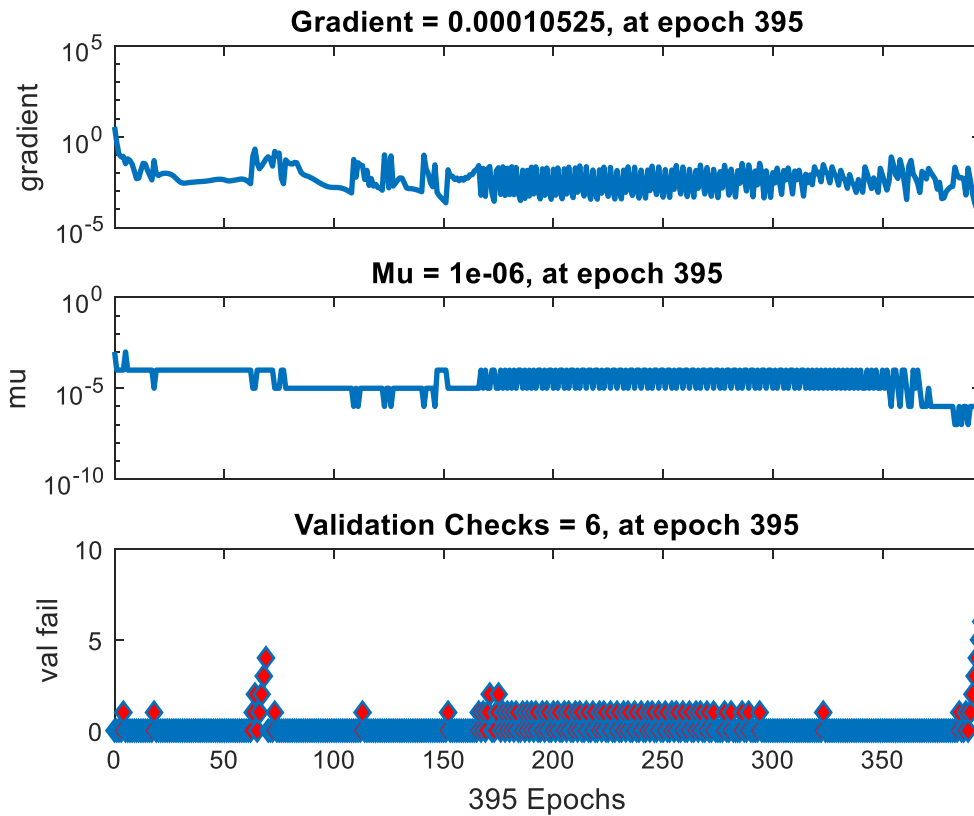
Figure 8. Denotes performance profiles for the LM trained network.
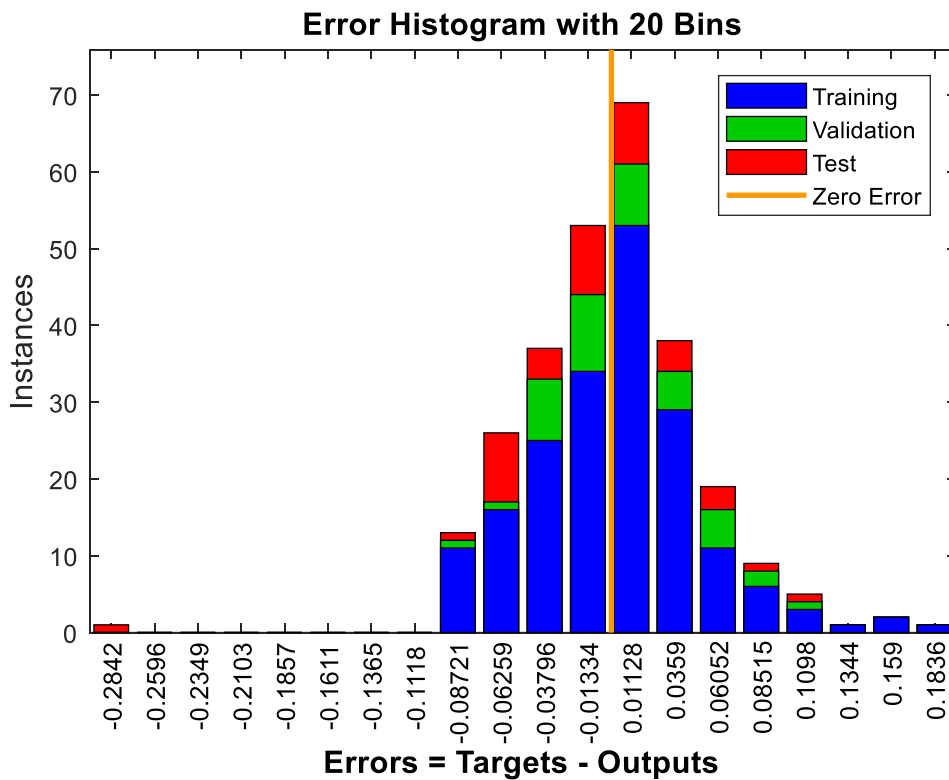
Figure 9. Error histogram of training, validation, and testing for the LM algorithm.

**4.5.2 Assessment of the ANN model robustness**

The experimental results and the predicted pile load-settlement are presented and discussed in this section. A series of experimental pile load-settlement were performed on open-ended steel piles. The testing program encompassed of three piles with aspect ratios (lc/d) of 12, 17 and 25 with 40mm diameter. It can be observed that all pile load-displacement curves failed by punching shear. The results of the pile-load tests indicate that the pile bearing capacity increased with increase in the sand relative density and the pile penetrated depth. This can be attributed due to an increase in the skin friction resistance and the point bearing developed in the effective zone. In total, 274 dataset were recorded the experimental pile load tests. Figures 10, 11 and 12 illustrate the distributions of the measured versus predicted load carrying capacity. It can be seen that plastic mechanisms in the soil surrounding the pile is the main cause for the non-linearity associated of the load-displacement response; as the applied load increases. The results revealed that there was an excellent correlation between the experimental and computational pile load-test results, with a correlation coefficient of 0.99 for validation dataset, which verified that the employed LM trained algorithm, could efficiently predict the pile load-settlement behaviour.
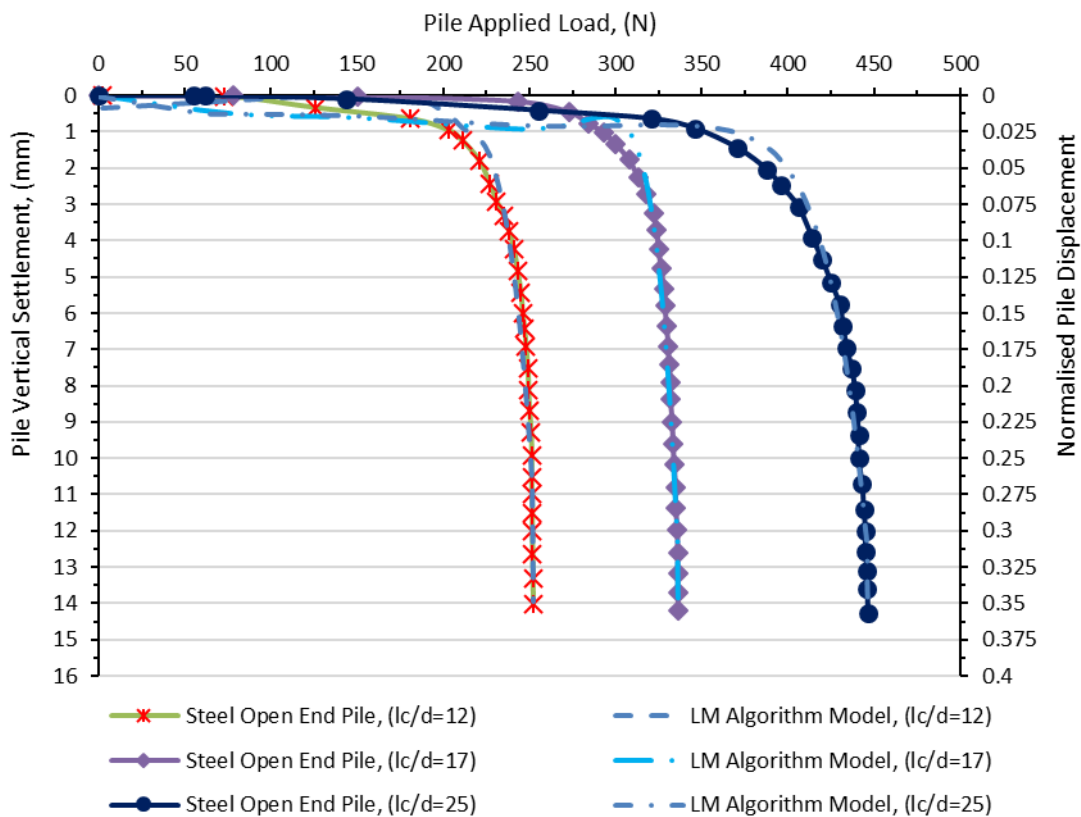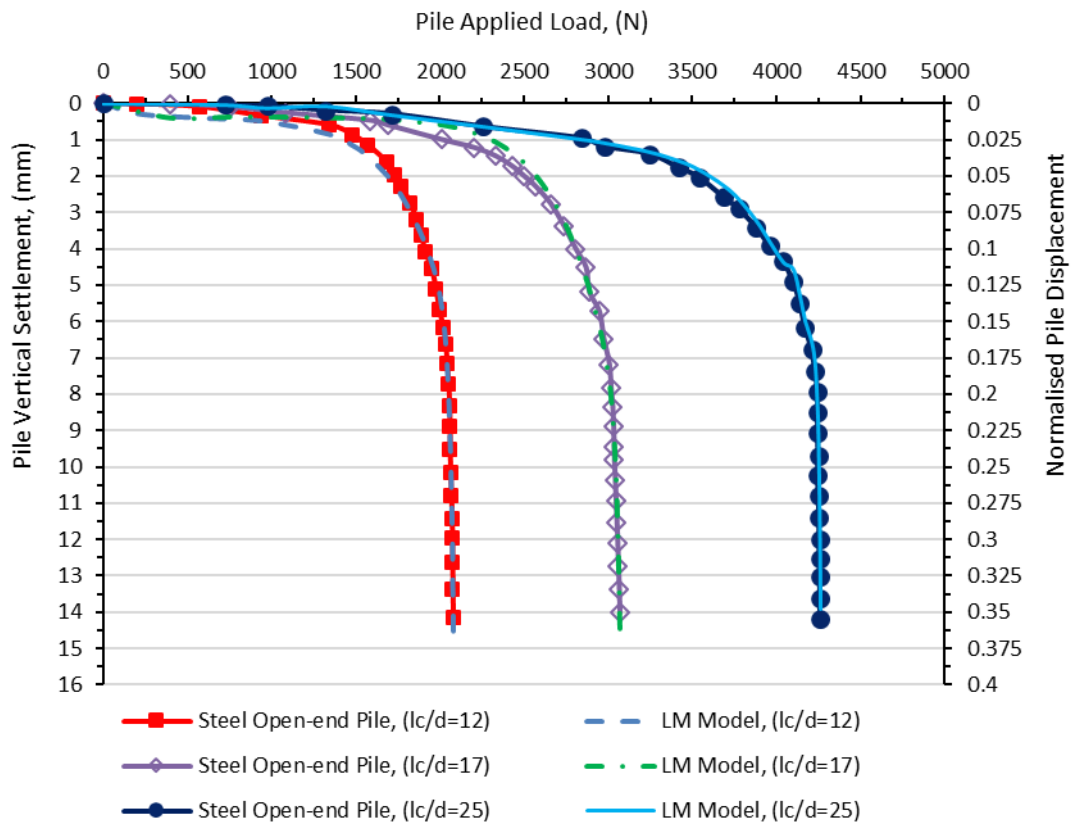


Figure 10. Experimental versus predicted pile load tests for steel piles tested in loose sand.
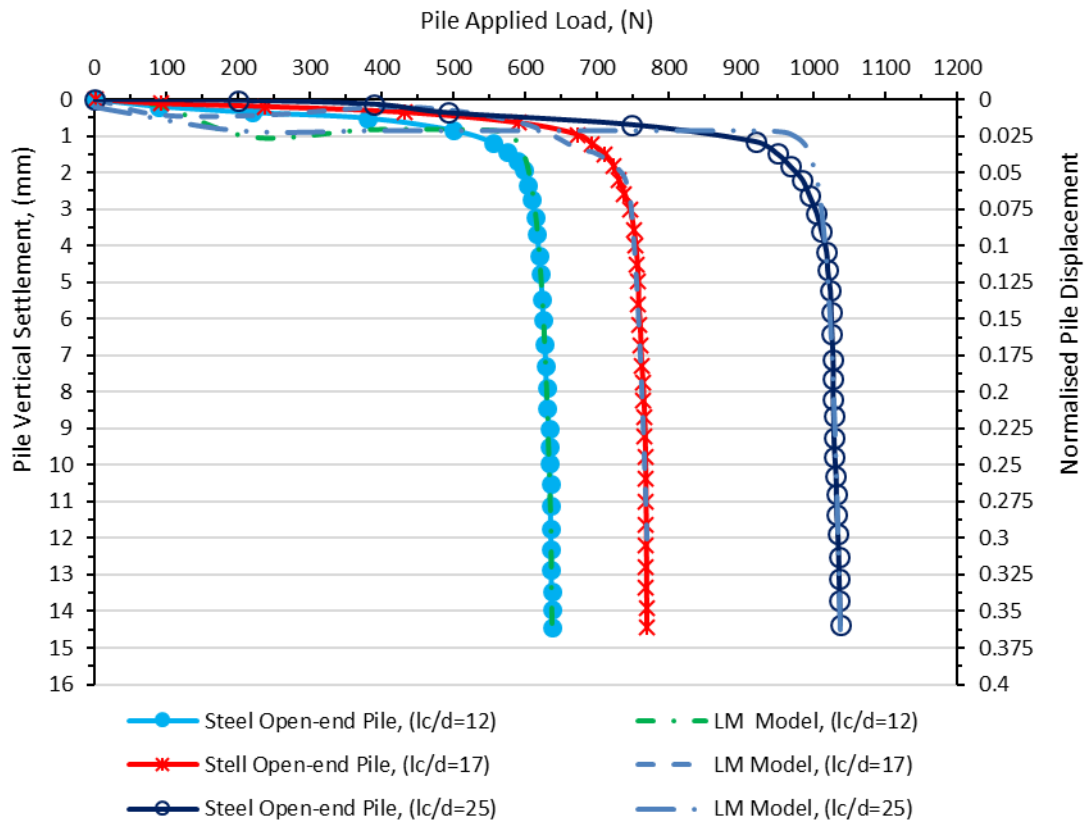
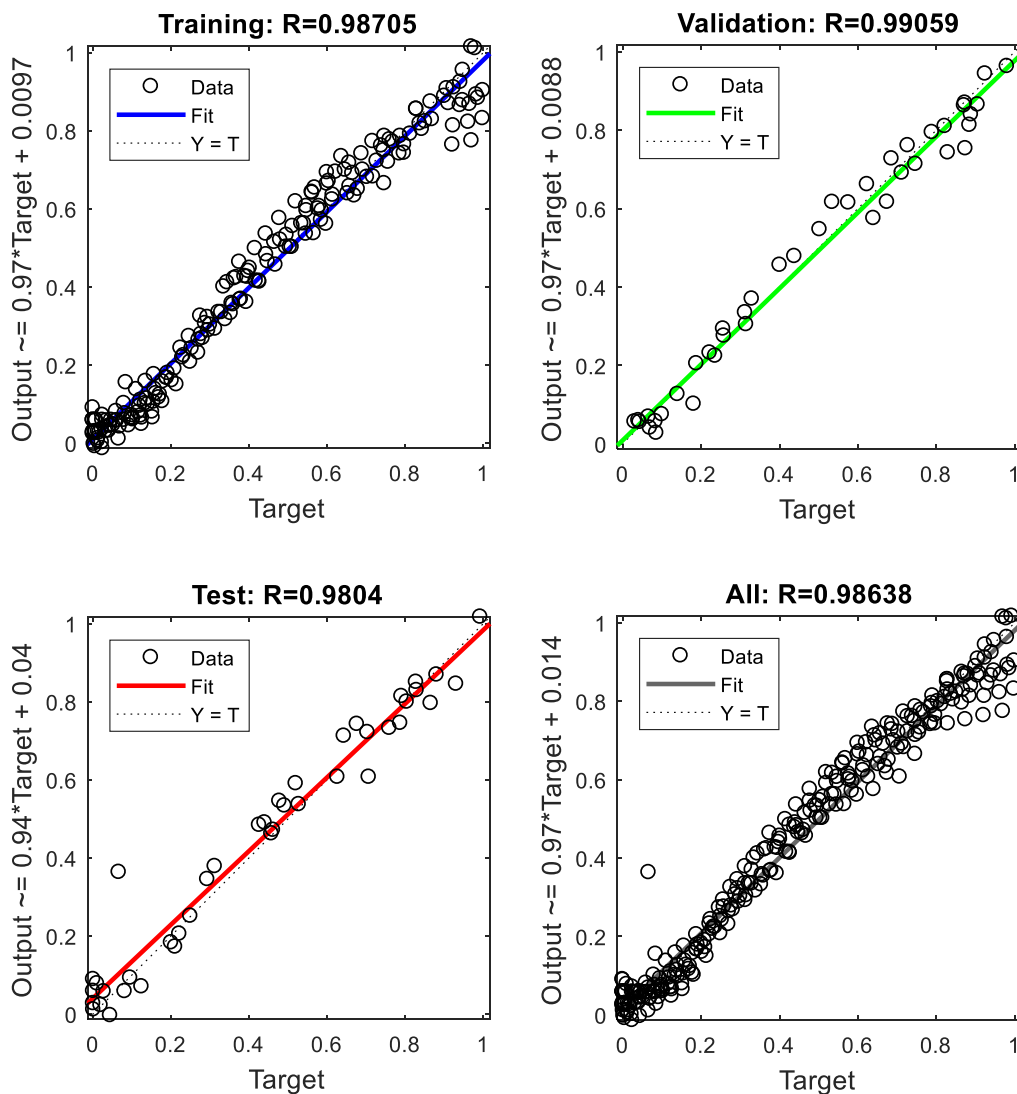Figure 11. Experimental versus predicted pile load tests for steel piles tested in medium sand.



Figure 12. Experimental versus predicted pile load tests for steel piles tested in dense sand.

405    A comparison has also been made between the targeted versus predicted pile corresponding settlement with

406    respect to the regression profile trends for the training, validation, testing and the complete dataset. As clearly

407    presented in Figure 13, the best-fit lines between the measured and predicted values can be seen with correlation

408    coefficients of 0.987, 0.99, 0.98 and 0.986 for training, testing, validation, and all data, demonstrating that the

409    newly implemented LM algorithm is a powerful data-driven tool and behaves in a fashion as would be expected.

410



411

412    Figure 13. Regression graphs of the experimental against predicted pile settlement for the training, validation,

413                                              testing and all data.

414

415   Furthermore, the validation dataset has been individually explored as recommended by Shahin and Jaksa (2005);

416   Jebur et al. (2018a) for further performance authentication and testing of the LM algorithm metric efficiency with

417   a 95% confidence interval (CI). It should be noted that a new MATLAB algorithm has been developed and used

418   to achieve the planned target. See supplementary information (Appendix C). remarkable consistency can be

419   observed, as shown in Figure 14, between the actual versus predicted pile settlement, with a coefficient of

420   correlation (R) and a root mean square error (RMSE) of 0.99 and 0.0437, thus in parallel with scatter index (SI)

421   of 0.349, and relatively insignificant BIAS value of 0.00071, respectively.

422
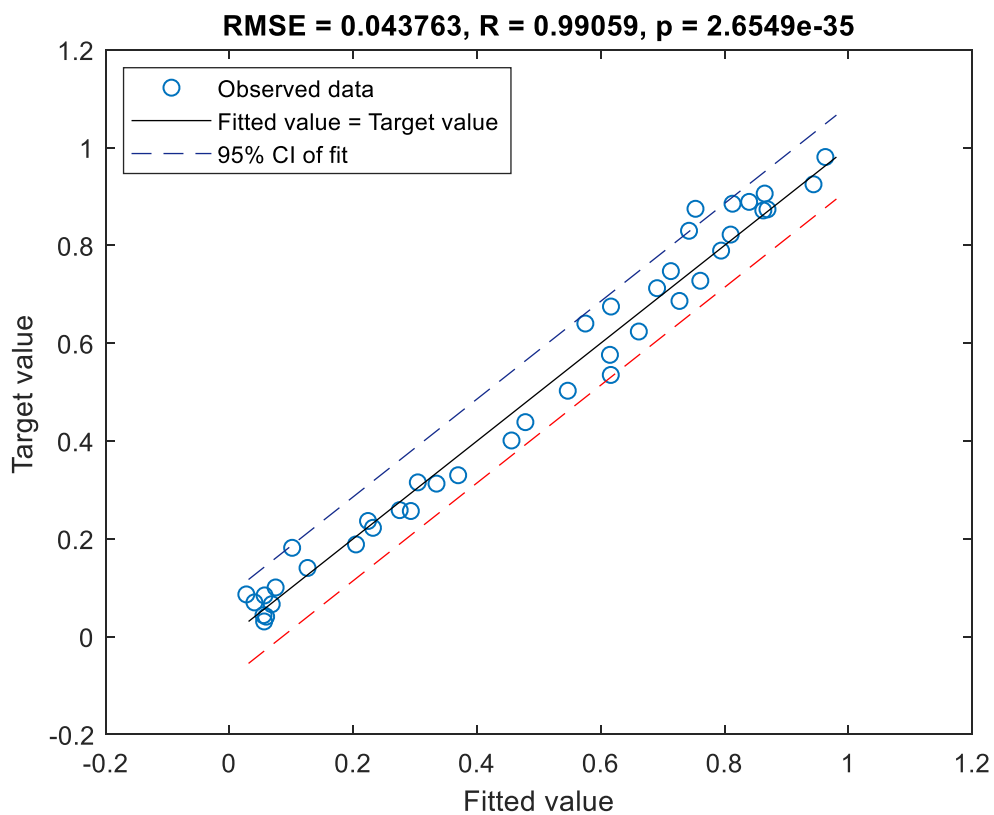


423

424          Figure 14. Fitted versus observed settlement at a 95% confidence interval (CI).

425

426   **4.6  Assessment of the ANN model performance with the various traditional methods**

427   A comparison has been made, in this part of the current study, to assess the roubstnace and the reliability of the

428   implemented approach with the traditional approaches currently used in the absence of pile load-test results,  as

429   recommended by: Poulos and Davis (1980); Vesic (1977) and Das (1995). As stated previously, the validation

430   subset was allocated to investigate the generalization ability of the trained LM algorithm. However, the validation

431 data subset was utilised in this comparison to evaluate the superiority of the developed ANN algorithm with the

432 aforementioned traditional methods.

433

### 4.6.1 Poulos and Davis (1980) approach

435 Poulos and Davis (1980) reported that the developed emperical equations can be used to predict pile(s) settlement

436 for single piles subjected to axial load as follows:

437

$$s = \frac{PI}{E_s D} \tag{16}$$

$$I = I_0 R_k R_h R_v \tag{17}$$

438

439 $P, E_s$ and $D$ are pile applied load, soil modulus of elasticity and pile diameter. I is the pile settlement influence

440 factor, which involves the soil depth, pile compressibility and Poisson's ratio $v$. $R_h$ is the influence element for

441 finite-depth, $R_v$ is the Poissons's ratio adjustment parameter, those influence parameters could be determined

442 using a series of design charts suggested by Poulos and Davis (1980). It is worth addressing that, if a rigid pile

443 driven in a semi-infinite soil with about 0.5 Poisson's ratio, $I_0$ is the only influence parameter need to be considered

444 in the equation and the rest of the parameters are assumed constant (Baziar et al., 2015).

445

### 4.6.2 Vesic (1977) approach

447 Vesic (1977) proposed that pile settlement can be calculated from the summation of three components

448 $s_1,$ $s_2$ and $s_3$ using the following simplified procedures.

$$S_1 = \frac{(P_{wp} + \xi P_{ws})L}{A_{tip}E} \tag{18}$$

$$S_2 = C_p \frac{P_{wp}}{dq_p} \tag{19}$$

$$S_3 = C_s \frac{P_{ws}}{Lq_p} \tag{20}$$

449 $P_{wp}$ is the pile applied load, $P_{ws}$ is the load transfierd by skin resistance and $\xi$ is the skin friction influence factor.

450 $C_p$ is an emperical parameter. The following equations can be applied to determine the $q_p$ and $C_s$ coefficents:

451

$$q_p = 40\frac{N_{tip}l}{d} \leq 400N_{tip}(kPa) \tag{21}$$

$$C_s = \left(0.93 + 0.16\sqrt{\frac{l}{d}}\right)C_p \tag{22}$$

The factor $\xi$ can be assumed to equal 0.5 and the parameter $C_p$ is equal to 0.09, as recommended for cohessionless soil (Poulos and Davis, 1980).

### 4.6.3 Das (1995) approach

The method offered by Das (1995) is the similar as that proposed by Vesic (1977) with some modifications in calculating $S_2$ and $S_3$ as stated below:

$$S_2 = \frac{P_{wp}D}{A_{tip}E_s}(1 - v^2)I_p \tag{23}$$

$$S_3 = \left(\frac{P_{ws}}{Ol_{penetarted}}\right)\left(\frac{d}{E_s}\right)(1 - v^2)I_{ps} \tag{24}$$

$$I_{ps} = 2 + 0.35\sqrt{\frac{l_{penetrated}}{d}} \tag{25}$$

where $I_p$ is equal to 0.88 as recommended for a circular cross-sectional pile Poulos and Davis (1980).

### 4.6.4 McVay et al. (1989) approach

McVay et al. (1989) proposed a non-linear method known as *t-z* curves, which could be utilized for load-displacement analysis of single piles. This method has been adopted by previous researchers (Zhang et al., 2008; Ismail, 2017). In this approach, the total pile settlement resulted from shaft and pile base, can be determined according to the following equations:

$$\text{Shaft:} z_s = \frac{r_0\tau_0}{G_{ib}}\left[\ln\frac{r_m - \omega}{r_0 - \omega} + \frac{\omega(r_m - r_0)}{(r_0 - \omega)(r_m - \omega)}\right] \tag{26}$$

$$\text{Base:} z_b = \frac{q_bA_b(1 - v)}{4r_0G_{ib}\left[1 - R_f\frac{q_b}{q_{max}}\right]^2} \tag{27}$$

470    in which $z_s$ and $z_b$ are, respectively, the settlement of pile shaft and pile base; $r_0$ is pile radius, ; $\tau_0$ is the shear

471    stress at the pile-soil interface, and $G_{ib}$ is the soil shear modulus at low strain; $r_m$ is the pile radius of influence;

472    $q_b$ and $q_{max}$ are the mobilised base resistance, and ultimate base base resistance. $\omega$ can be defined as follows:

473

$$\omega = \frac{r_0 \tau_0 R_f}{\tau_{max}} \tag{28}$$

474    From the above expression (Eq. 28), it is clear that the t-z method for both components are developed according

475    to the limiting values of pile shaft, pile base resistance, and the soil elastic modulus. In the context of this study,

476    the limiting values of pile shaft and pile base resistance are predicted following the recommendations specified

477    by Meyerhof (1976).  This is in agrement with the approach utilised by Ismail (2017).

478

479    With the aim of further examining the validity of the proposed ANN model, Figure 15 characterises graphical

480    comparisons between the measured pile settlement and with those given by the most conventional methods as

481    outlined previously, which are normally used in the absence of the in-situ load carrying capacity test. The

482    comparative results indicated that the aforementioned design methods are not reliable to simulate pile load-

483    settlement and they need to be revised, if employed, in future applications. This can be probably assigned to serval

484    various hypotheses associated with the soil-pile interaction. The results also revealed that the non-linear

485    approaches set out by Fleming (1992) and McVay et al. (1989) provide better results when compared to elastic

486    methods. As depicted, the computational results are in remarkable agreement with the measured pile-load

487    settlement responses, suggesting that the LM algorithm is highly successful in simulating the full response of load

488    carrying capacity with obvious advantages.

489

490    ## 5. Scale factor

491    According to the geotechnical scaling standards reported by Wood (2004), Eq. (29) can be utilised when the

492    stiffness modulus of the sand in the effective stress zone and in the situ is about the same.

493

$$E_m I_m = \frac{1}{n^4} E_p I_p \tag{29}$$

494

495    where $E_m I_m$ stand for the model pile elastic modulus (GPa), and moment of inertia (m$^4$), $n^4$ is the scaling factor,

496    and EpIp is the elastic modulus, and moment of inertia for the prototype pile. The pile diameter used in the

497 experiment is 40 mm and having different aspect ratios as stated previously. The diameter for the range of the

498 prototypes piles were selected as 0.3m diameter, with length of 12m for steel piles. The elastic modulus, E for

499 both the prototype and the steel model pile where chosen to have the same value 200 GPa (Gere and Timoshenko,

500 1997). According to Eq. 26, the scale factor (n) for prototype steel pile is 20, 16.8, and 14 for slenderness ratios

501 of 12, 17, and 25.

502
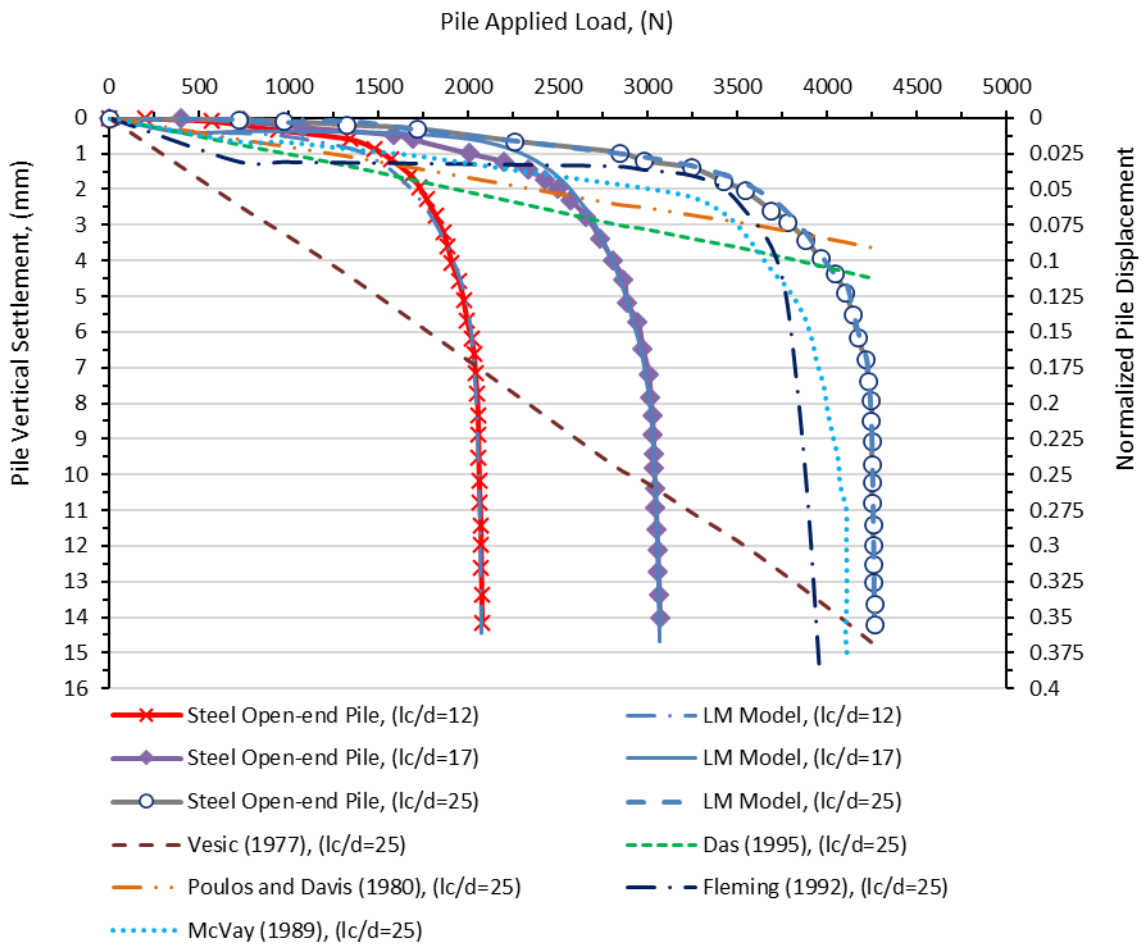


503

504 Figure 15. Measured versus predicted pile load-settlement for the proposed LM compared with other
505 conventional methods.

506

507

508

509

510

511

512

## 6. Conclusions

The current study targeted at developing and verifying a new data-driven artificial intelligence approach using the Levenberg-Marquardt (LM) approach, based on the MATLAB environment that can be successfully applied to simulate the load-settlement response of steel piles, covering different sand relative densities. The conventional design procedure proposed by Poulos and Davis (1980); Vesic (1977); Das (1995); Fleming (1992); and McVay et al. (1989) were utilised for comparisons purposes. the following conclusions can be drawn:

- Pile bearing capacity in dense sand is substantially greater than for those embedded in loose and medium sand. This can be assigned to an increase in the end bearing capacity and shaft resistance developed in the effective soil-pile penetration depth.

- The pile load-settlement results are idealistic for pile foundations under axial loads, i.e., reducing from pile head to pile toe due to the increase in the developed shaft resistance and the point bearing in the soil effective zone.

- Substantial agreement has been identified between the measured and the computational values of the pile-load tests, demonstrating that the LM algorithm is efficient and an appropriate approach to predict pile load-settlement. This was confirmed with RMSE, R and MAE of 0.043, 0.99, and 0.0019, thus with a relatively low percentage error of SI and BIAS at 0.349, and 0.00071, correspondingly.

- The optimal LM algorithm structure was idintifed at a topology of 5:10:1 with a tangent sigmoid *"tansig"* transfer function between input and hidden layer and linear *"purelin"* transfer function between the hidden and output layer.

- According to the sensitivity analysis and the statistical statistical significance model, five parameters namely, applied load (P), pile slenderness ratio ($l_c/d$), pile axial rigidity (EA), pile effective length ($l_c$) and sand-pile friction angle ($\delta$) were identified to play a substantial role on pile capacity and the corresponding settlement, at varying contribution level following the order P (0.804) > $\delta$ (0.711) > lc/d (0.119) > 1 (0.88) > EA (0.015).

- The statistical analysis results revealed that the maximum detected MDs for five IVs was found to be 17.63 that is less than the maximum value (20.52), which confirm the absence of outliers in the dataset being studied.

- The adopted LM algorithm has several favourable features (i.e. generalization ability, efficiency and ease of application) which make it a good choice to model the complex nonlinear system.

- To reveal the applicability of the LM algorithm, a graphical performance comparison was made between the applied LM algorithm and conventional methods. Based on the outcomes, the adopted LM training algorithm is substantially superior the traditional empirical relationships and has been identified to provide better solutions as confirmed by the performance skills metric, which demonstrates the applicability of the implemented algorithm and its potential in future applications.

The main limitation of this study lies in the fact that the piles were tested in cohesionless soil. Considering this limitation, the feasibility of the proposed LM training algorithm to capture the full load-settlement response for model piles embedded in cohesion soil will be examined in the future. In addition, more data should be included as the measured load-settlement (l-s) curves in Figure 15 contain both the training and testing dataset.

# References

Abdellatif M., Atherton W., Alkhaddar R. & Osman Y. (2015) "Flood risk assessment for urban water system in a changing climate using artificial neural network". *J, Nat Hazards* 79**,** 1059–1077.

Abdellatif M.E.M. (2013) "Modelling the Impact of Climae Change on Urban Drainage System". *Ph.D thesis, Department of Built Environment, Liverpool John Moores University, UK*.

Akdag C.T. & Özden G. (2013) "Nonlinear behavior of reinforced concrete (RC) and steel fiber added RC (WS-SFRC) model piles in medium dense sand". *Construction and Building Materials* 48**,** 464-472.

Al-Gburi M., Jonasson J. & Nilsson M. (2016) "Prediction of restraint in second cast sections of concrete culverts using artificial neural networks". *European Journal of Environmental and Civil Engineering,* 22**,** https://doi.org/10.1080/19648189.2016.1186116, 226–245.

Alrashydah E.I. & Abo-Qudais S.A. (2018) "Modeling of creep compliance behavior in asphalt mixes using multiple regression and artificial neural networks". *Construction and Building Materials,* 159**,** 635-641.

Ardakani A. & Kordnaeij A. (2017) "Soil compaction parameters prediction using GMDH-type neural network and genetic algorithm". *European Journal of Environmental and Civil Engineering***,** http://dx.doi.org/10.1080/19648189.2017.1304269, 1-14.

Asteris P.G., Kolovos K.G., Douvika M.G. & Roinos K. (2016) "Prediction of self-compacting concrete strength using artificial neural networks". *European Journal of Environmental and Civil Engineering,* 20**,** 102-122.

Baziar M.H., Azizkandi A.S. & Kashkooli A. (2015) "Prediction of Pile Settlement based on Cone Penetration Test Results: An ANN Approach". *KSCE Journal of Civil Engineering,* 19(1)**,** 98-106.

Bowles J.E. (1978) "Engineering properties of soils and their measurement". *2nd ed. New York (NY): McGraw-Hill International. Book Company***,** 213.

BSI (BS EN 1377-7:1990) "Methods of test for soils for civil engineering purposes Part 7: Shear strength tests". *BSI, London, UK*.

BSI (BS EN 8004:1986) "Code of practice for foundations". *BSI, London, UK*.

Chen Y. & Kulhawy F.H. (2002) "Evaluation of drained axial capacity of drilled shafts, in: Proc., Deep Foundations 2002". *Geotech. Spec. Publication No. 116, vol. 2, ASCE***,** 1200–1214.

Cho G.C., Dodds J. & Santamarina J.C. (2006) "J Geotech Geoenviron Eng". *Particle shape effects on packing density, stiffness, and strength: natural and crushed sands,* 132**,** 591–602.

Cho S.E. (2009) "Probabilistic stability analyses of slopes using the ANN-based response surface". *Journal of Computers and Geotechnics***,** 787–797.

Das B.M. (1995) "Principles of foundation engineering, third edition". *Boston ua PWS Publ. Co*.

Deo R.C. & Şahin M. (2015) "Application of The Extreme Learning Machine Algorithm for the Prediction of Monthly Effective Drought Index in Eastern Australia". *Atmospheric Research 153***,** 512–525.

Derbal I., Bourahla N., Mebarki A. & Bahar R. (2017) "Neural network-based prediction of ground time history responses". *European Journal of Environmental and Civil Engineering***,** https://doi.org/10.1080/19648189.2017.1367727, 1-18.

Dyskin A.V., Estrin Y., Kanel-Belov A.J. & Pasternak E. (2001) "Toughening by fragmentation—how topology helps". *Adv Eng Mater,* 3**,** 885–888.

Erdal H.I. ( 2013) "Two-level and hybrid ensembles of decision trees for high performance concrete compressive strength prediction". *Engineering Applications of Artificial Intelligence 26 (7)***,** 1689–1697.

Fellenius B.H. (1988) "Unified design of piles and pile groups". *Transportation Research Record* 1169, 75-81.

Fleming W.A. (1992) "new method of single pile settlement and analysis. Geotechnique". 42(3), 411–425.

Gere J.M. & Timoshenko S.P. (1997) "Mechanics of materials ". 912 p. 4th eddition

Harandizadeh H., Toufigh M.M. & Toufigh V. (2018) "Different Neural Networks and Modal Tree Method For Predicting Ultimate Bearing Capacity of Piles". *IUST,* 8, 311-328.

Ismail A. (2017) "ANN-based empirical modelling of pile behaviour under static compressive loading". *Front. Struct. Civ. Eng.*, https://doi.org/10.1007/s11709-017-0446-2, 1-15.

Jardine R.J. & Chow F.C. (2007) "Some Recent Development in Off-shore Pile Design". *6th int. Offshore Site Investigation Geotechnics Conf., London*.

Jebur A.A., Atherton W. & Al Khaddar R.M. (2018a) "Feasibility of an evolutionary artificial intelligence (AI) scheme for modelling of load settlement response of concrete piles embedded in cohesionless soil". *Ships and Offshore Structures, 10.1080/17445302.2018.1447746,* 13, 705-718.

Jebur A.A., Atherton W., Alkhadar R.M. & Loffill E. (2017) "Piles in sandy soil: A numerical study and experimental validation". *Procedia Engineering 196*, 60-67.

Jebur A.A., Atherton W., Khaddar R.M.A. & Loffill E. (2018b) "Settlement Prediction of Model Piles Embedded in Sandy Soil Using the Levenberg–Marquardt (LM) Training Algorithm". *Geotechnical and Geological Engineering*, https://doi.org/10.1007/s10706-018-0511-1,1-14.

Jeong D.-I. & Kim Y.-O. (2005) "Rainfall-runoff models using artificial neural networks for ensemble stream flow prediction". *Hydrol Process* 19(19), 3819–3835.

Józefiak K., Zbiciak A., Maślakowski M. & Piotrowski T. (2015) "Numerical Modelling and Bearing Capacity Analysis of Pile Foundation". *Procedia Engineering,* 111, 356-363.

Juncai X., Qingwen R. & Zhenzhong S. (2015) "Prediction of the Strength of Concrete Radiation Shielding Based on LS-SVM". *Annals of Nuclear Energy 85*, 296–300.

Lehane B.M. & Gavin K.G. (2001) "Base resistance of jacked pipe piles In sand". *Journal Of Geotechnical And Geoenvironmental Engineering* 127, 473-480.

Łodygowski T. & Sumelka W. (2006) "Limitations in Application of Finite Element Method in Acoustic Numerical Simulation". *J. Theor. Appl. Mech, 44(4)*, 849-865.

Loria R.A.F., Orellana F., Minardi A., Fürbringer J. & Laloui L. (2015) "Predicting the axial capacity of piles in sand". *Computers and Geotechnics,* 69, 485-495.

Majeed A.H., Mahmood K.R. & Jebur A.A. (2013) "Simulation of Hyperbolic Stress-Strain Parameters of Soils Using Artificial Neural Networks". *Proccedings of the 23rd International Conference on Geotechnical Engineering; Feb 21st - 23rd; Hammamet, Tunisia*, 105-115.

Masters T. (1993) "PracticalNeuralNetworkRecipesinC++. Academic". *San Diego*.

McVay M., Townsend F.C., Bloomquist D.G., O'Brien M.O. & Caliendo J.A. (1989) "Numerical analysis of vertically loaded pile groups". *In: Proceedings of the Foundation Engineering Congress, North Western University, Illinois. USA*, 675–690.

Meyerhof G.G. (1976) "Bearing Capacity and Settlement of Pile Foundations". *ASCE, Journal of Geotechnical Engineering, 102(GT3)*, 197-228.

Momeni E., Nazir A., Armaghani D.J. & Maizir H. (2014) "Prediction of pile bearing capacity using a hybrid genetic algorithm-based ANN". *Measurement,* 57, 122-131.

Murthy V.N.S. (2002) "Principles and Practices of Soil Mechanics and Foundation Engineering". *Marcel Dekker Inc, Florida, USA.*

Najafzadeh M. (2015) "Neuro-fuzzy GMDH systems based evolutionary algorithms to predict scour pile groups in clear water conditions". *Ocean Engineering,* 99**,** 85-94.

Najafzadeh M., Balf M.R. & Rashedi E. (2016) "Prediction of maximum scour depth around piers with debris accumulation using EPR, MT, and GEP models". *Journal of Hydroinformatics,* doi: 10.2166/hydro.2016.212**,** 867-884.

Najafzadeh M., Saberi-Movahed F. & Sarkamaryan S. (2017) "NF-GMDH-Based self-organized systems to predict bridge pier scour depth under debris flow effects". *Marine Georesources & Geotechnology***,** 1-14.

Nguyen-Truong H.T. & Le H.M. (2015) "An Implementation of the Levenberg–Marquardt Algorithm Forsimultaneous-Energy-Gradient Fitting Using Two-Layer Feed Forwardneural Networks". *Chemical Physics Letters* 629**,** 40-45.

Pallant J. (2005) "SPSS Survival Manual. Allen & Unwin, Australia.".

Poulos H.G. & Davis E.H. (1980) "Pile Foundation Analysis and Design". *John Wiley & Sons, New York.*

Rafiq M.Y., Bugmann G. & Easterbrook D.J. (2001) "Neural network design for engineering applications". *Comput Struct* 79**,** 1541-1552.

Rajesh R. & Prakash J.S. (2011) "Extreme learning machines—a reviewand stateof- the-art". *Int. J.Wisdom Based Comput. 1***,** 35–49.

Reddy K.M. & Ayothiraman R. (2015) "Experimental Studies on Behavior of Single Pile under Combined Uplift and Lateral Loading". *Journal of Geotechnical and Geoenvironmental Engineering,* 141**,** 1-10.

Reese L.C., Isenhower W.M. & Wang S.T. (2006) "Analysis and design of shallow and deep foundations". *John Wiley & Sons, New Jersey.*

Remaud D. (1999) "Pieux Sous Charges Latérales: Etude Expérimentale De L'effet De Groupe". *PhD thesis. Université de Nantes; French.*

Rezaei H., Nazir R. & Momeni E. (2016) "Bearing capacity of thin-walled shallow foundations: an experimental and artificial intelligence-based study". *J of Zhejiang University-SCIENCE A (Applied Physics & Engineering), 17(4)***,** 273-285.

Schawmb T. (2009) "The Continuous Helical Displacement pile in comparison to conventional piling techniques". *Masters Thesis. University of Dundee, UK.*

Shahin M.A. & Jaksa M.B. (2005) "Neural network prediction of pullout capacity of marquee ground anchors". *Journal of Computers and Geotechnics 32***,** 153-163.

Shawash J. (2012) "Generalised Correlation Higher Order Neural Networks, Neural Network operation and Levenberg-Marquardt training on Field Programmable Gate Arrays". *PhD thesis. Department of Electronic and Electrical Engineering, , University College London, UK.*

Tabachnick B.G. & Fidell L.S. (2013) "Using Multivariate Statistics". *Sixth Edition, Allyn and Bacon, Boston.*

Tarawneh B. (2017) "Predicting standard penetration test N-value from cone penetration test data using artificial neural networks". *Geoscience Frontiers* 8**,** 199-204.

Taylor R.N. (1995) "Geotechnical Centrifuge Technology". *First ed., Chapman & Hall, London.*

Tschuchnigg F. & Schweiger H.F. (2015) "The embedded pile concept – Verification of an efficient tool for modelling complex deep foundations". *Computers and Geotechnics,* 63**,** 244-254.

692  Ueno K. (2000) "Methods for preparation of sand samples centrifuge". *In: Proceedings of the International*
693     *Conference Centrifuge 98. Tokyo, Japan, Taylor and Francis***,** 23-25.

694  Vesic A.S. (1967) "Ultimate Load and Settlement of Deep Foundations in Sand". *Proceedings of the Symposium*
695     *on Bearing Capacity and Settlement of Foundations*.

696  Vesic A.S. (1977) "Design of pile foundations". *National cooperative highway research program, synthesis of*
697     *practice No. 42. Washington, DC: Transportation Research Board*.

698  Walfish S. ( 2006) "A review of statistical outlier methods". *Pharm. Technol* 30**,** 82-86.

699  Wilamowski B.M. & Yu H. (2010) "Improved cpmputaion for Levenberg-Marquardt". *IEEE Transaction on*
700     *Neural Network, (21)***,** 930-737.

701  Wood D.M. (2004) "Geotechnical Modelling". *Spon Press, Taylor and Francis Group,* United States of America.

702  Yadav A.K., Malik H. & Chandel S.S. (2014) "Selection of most relevant input parameters using WEKA for
703     artificial neural network based solar radiation prediction models". *Renewable and Sustainable Energy*
704     *Reviews,* 31**,** 509-519.

705  Zhang L.M., Xu Y. & Tang W.H. (2008) "Calibration of models for pile settlement analysis using 64 field load
706     tests". *Canadian Geotechnical journal,* 45(1)**,** 59-73.

707